Hindawi
Journal of Advanced Transportation
Volume 2019, Article ID 8469316, 15 pages
https://doi.org/10.1155/2019/8469316

Research Article

Extracting Origin-Destination with Vehicle Trajectory Data and Applying to Coordinated Ramp Metering

Cheng Zhang[1], **Jiawen Wang**[2], **Jintao Lai**[1], **Xiaoguang Yang**[1], **Yuelong Su**[3] and **Zhenning Dong**[3]

[1] *The Key Laboratory of Road and Traffic Engineering, Ministry of Education, Tongji University, 4800 Cao'an Road, Shanghai 201804, China*
[2] *Department of Traffic Engineering, University of Shanghai for Science and Technology, 516 Jungong Road, Shanghai 200093, China*
[3] *AutoNavi Software Co., Beijing 100102, China*

Correspondence should be addressed to Jiawen Wang; wangjw@usst.edu.cn

Received 8 January 2019; Revised 18 April 2019; Accepted 12 June 2019; Published 8 July 2019

Academic Editor: Zhi-Chun Li

Ramp metering is an effective measure to alleviate freeway congestion. Traditional methods were mostly based on fixed-sensor data, by which origin-destination (OD) patterns cannot be directly collected. Nowadays, trajectory data are available to track vehicle movements. OD patterns can be estimated with weaker assumptions and hence closer to reality. Ramp metering can be improved with this advantage. This paper extracts OD patterns with historical trajectory data. A validation test is proposed to guarantee the sample representativeness of vehicle trajectories and then implement coordinated ramp metering based on the contribution of on-ramp traffic to downstream bottleneck sections. The contribution is determined by the OD patterns. Simulation experiments are conducted under real-life scenarios. Results show that ramp metering with trajectory data increases the throughput by another 4% compared with traditional fixed-sensor data. The advantage is more significant under heavier traffic demand, where traditional control can hardly relieve the situation; in contrast, our control manages to make congestion dissipate earlier and even prevent its forming in some sections. Penetration of trajectory data influences control effects. The minimum required penetration of 4.0% is determined by a t-test and the Pearson correlation coefficient. When penetration is less than the minimum, the correlation between the estimation and the truth significantly drops, OD estimation tends to be unreliable, and control performance becomes more sensitive. The proposed approach is effective in recurrent freeway congestion with steady OD patterns. It is ready for practice and the analysis supports the real-world application.

1. Introduction

Ramp metering has been proved to be an effective measure to relieve freeways congestion. It regulates the traffic volume at entry ramps with traffic signals, to keep the mainline traffic operating at the desired level and avoid capacity drop [1]. Proper entry control reduces the probability of breakdowns on the mainline while also considering the throughput of other traffic [2].

Researches on ramp metering can be dated back to 1965 when Wattleworth first proposed a linear programming model to generate a fixed-time control scheme to alleviate peak-hour freeway congestion with static origin-destination (OD) information [3]. With real-time measurement available, reactive ramp metering strategies have been proposed. The best-known strategies are the demand-capacity (DC) strategy, the occupancy (OCC) strategy, and the ALINEA. DC strategy allowed ramp volume to make up the difference between the estimated capacity of mainline and measured upstream volume. OCC strategy calculated the metering rate by comparing the measured occupancy and the target value [4]. ALINEA was a feedback regulator, aiming to maintain capacity flow downstream of the merge area [5]. All these three strategies are local ramp metering based on simple logic. Field results showed their effectiveness [6]. Some extension versions were also proposed such as PI-ALINEA [7] and ITC-ALINEA [8]. They belong to local ramp metering strategies.

Coordinated ramp metering considers coordination among ramps. Cooperative algorithms, such as HELPER [9] and HERO [10], determined critical ramps whose downstream mainline sections are in most serious congestion and then force its upstream on-ramps to reduce metering rates accordingly. Bottleneck algorithms, such as FLOW [11], ZONE [12], and SWARM [13], calculated metering rates based on volume reduction in the mainline bottleneck. The above two kinds of algorithms are rule-based ones. The logic is like "*IF traffic condition, THEN control scheme*", which is easy to implement.

Another kind of coordinated ramp metering control is optimal control. Started in the 1960s, the optimizing models inputted historical data and outputted static or time-of-day control schemes [14]. In the 1990s, real-time measurements were considered. The approach used a rolling horizon to get a dynamic optimal control scheme [15]. Optimal control can generate the best solution in spite of complex modeling and computing. Among them, linear programming was relatively easy to solve, so it had been first developed and implemented [16]. Nonlinear relationships of traffic systems had also been discussed and applied to ramp metering [17].

A majority of these researches were based on macroscopic traffic models, including Cell Transmission Model [18], Payne–Whitham model [19], and METANET [20]. They adopted models to describe the relationships among variables and simulate the evolution of freeway systems. Artificial intelligence was also employed to ramp metering. These techniques included fuzzy logic [21], neural networks [22], iterative learning [8], and other heuristic methods [23].

For most coordinated ramp metering, origin-destination (OD) demand is a vital input. Traditionally, OD matrices were derived from surveys, which were time-consuming and usually not precise enough due to subjective response and small sample size. With the development of traffic detection technology, many methods were proposed to estimate OD with different data sources. Generally, they can be divided into two categories—the fixed-sensor-based methods and the trajectory-based ones.

Fixed sensors include loop detectors, radar detectors, and video sensors. They collect traffic information like volume, occupancy, and speed at certain locations. A lot of researches were conducted to estimate OD with fixed-sensor data. One of the most primitive approaches is proportional distribution method [24]. It regarded that the OD volume on freeways is in proportion to the volume at entrance ramps. Obviously, this assumption was too strong. A gravity-based model was then proposed [25]. It assumed that the trip distances meet Gamma distribution, which implied that too long or too short trips are of little possibility. Also, estimated travel time distributions were applied to OD matrix estimation [26]. Besides, commonly used models include generalized least square model [27], the maximum entropy model [28], and Bayesian theory [29]. Since fixed sensors cannot capture traffic's origin and destination, these methods had to introduce assumptions to estimate OD.

Trajectory data record the movement of individual vehicles and thus provide a more reliable data source for OD estimation. The first kind of data is returned by detectors on vehicles, such as floating car data collected by GPS equipment [30] and vehicle trajectory data returned by mobile navigation applications [31]. Since not all vehicles are equipped with GPS devices or not all travelers use navigation apps, this kind of data is sample data. Penetration rate influences estimation accuracy [32]. The second kind of data is collected by widely distributed fixed sensors, like automatic license plate recognition data [33] and Bluetooth and WiFi data [34]. Different from traditional fixed sensors, they identify each vehicle or traveler via an identification (ID), which makes trajectory reconstruction possible.

Nowadays high-quality trajectory data have become available. Previous researches have utilized trajectory data to estimate traffic state parameters such as OD flows [31], queue length [35], delay [36], and travel time [37]. Results showed that estimation accuracy was improved with trajectory data. If traffic parameters estimated by trajectory data could be applied to ramp metering, the control performance is supposed to be improved. However, limited research or practice has implemented it since high-quality trajectory data were not available. Low frequency (e.g., > 30 seconds of record interval) and low penetration (e.g., <10%) are usual situations. Thus, most existing ramp metering controls were still based on fixed-sensor data—typically loop detector data. The OD table was estimated by link counts [19]. Instead of estimating OD tables, some researches introduced off-ramp exit percentages to predict freeway flows [38]. Vehicles from different origins have the same probability to leave the mainline when they come to an off-ramp [39]. This assumption is not necessarily true. Others assumed that the OD flows were perfectly known and the studies were conducted under ideal scenarios [18]. However, these researches have a long distance from practice.

The contribution of this paper includes (1) proposing and implementing coordinated ramp metering with real trajectory data; (2) comparing the control performance of the proposed approach and the traditional method under different traffic demand intensity; (3) analyzing the influence of penetration rate on control performance and determining a minimum value. The remaining part of this paper is organized as follows: Section 2 introduces the bottleneck algorithm implemented in this research. Section 3 explains the process of weights calibration with trajectory data. Section 4 presents simulation experiments settings. Section 5 compares the experiment results. Section 6 analyzes the sensitivity on penetration rate. Section 7 concludes this paper.

2. Bottleneck Algorithm

The bottleneck algorithm is essentially a rule-based algorithm for coordinated ramp metering control. Ramp metering rates are calculated, respectively, on the basis of system capacity constraints and local conditions. The more restrictive metering rate is selected and finally adjusted to constraints including maximum queue length and minimum metering rate.

Figure 1 shows relevant variables of bottleneck sections and on-ramps. i is mainline section index, j is on-ramp index,

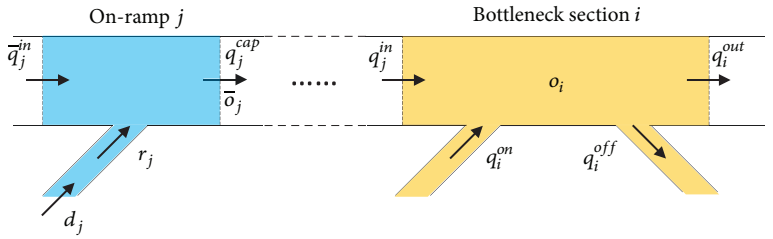

FIGURE 1: Ramp metering variables of bottleneck section i and on-ramp j.

and k is the time step. A mainline section i is defined as a bottleneck if its average occupancy o_i is over the threshold o_i^{thres} (see (1)); at the same time the total entering flow (including inbound flow q_i^{in} and on-ramp flow q_i^{on}) is more than the total exiting flow (including outbound flow q_i^{out} and off-ramp flow q_i^{off}) (see (2)).

$$o_i(k) > o_i^{thres} \tag{1}$$

$$q_i^{in}(k) + q_i^{on}(k) > q_i^{out}(k) + q_i^{off}(k) \tag{2}$$

A bottleneck metering rate r_j^B is calculated if there exists a bottleneck on the freeway. On the basis of the metering rate r_j in the last time step, entering traffic is reduced to alleviate congestion in bottleneck sections. The volume reduction is determined according to the law of traffic volume conservation. For bottleneck section i, its volume reduction q_i^{reduce} is the difference between the total entering flow and the total exiting flow (see (3)). Then the reduction is distributed to its area of influence, i.e., its upstream on-ramps according to weights $W_{j,i}$ (see (4)). The weights calculation is discussed in Section 3.4 in detail. When there are more than one bottlenecks, their areas of influence overlap. On-ramp volume reduction $q_{j,i}^{reduce}$ can be calculated from each bottleneck. The maximum volume reduction is used to calculate the bottleneck metering rate (see (5)).

$$\begin{aligned} q_i^{reduce}(k+1) = {} & \left[q_i^{in}(k) + q_i^{on}(k)\right] \\ & - \left[q_i^{out}(k) + q_i^{off}(k)\right] \end{aligned} \tag{3}$$

$$q_{j,i}^{reduce}(k+1) = q_i^{reduce}(k+1) \cdot W_{j,i} \tag{4}$$

$$r_j^B(k+1) = r_j(k) - \max_i \left[q_{j,i}^{reduce}(k+1)\right] \tag{5}$$

Then, a local metering rate r_j^L is calculated on the basis of the local condition of on-ramp j using demand-capacity strategy. To be specific, if the mainline occupancy downstream of the on-ramp $\overline{o}_j$ does not reach the threshold $\overline{o}_j^{thres}$, the metering rate is the difference between capacity q_j^{cap} and mainline traffic flow upstream of the on-ramp $\overline{q}_j^{in}$; otherwise, it equals the preset minimum value r_j^{min} (see (6)). The occupancy threshold $\overline{o}_j^{thres}$ is corresponding to the state when the mainline reaches capacity flow.

$$r_j^L(k+1) = \begin{cases} q_j^{cap} - \overline{q}_j^{in}(k), & \overline{o}_j(k) \le \overline{o}_j^{thres} \\ r_j^{min}, & \overline{o}_j(k) > \overline{o}_j^{thres} \end{cases} \tag{6}$$

If on-ramp j is the nearest on-ramp upstream of bottleneck section i, then the inbound flow upstream of the bottleneck section i equals mainline traffic flow upstream of the on-ramp j (see (7)). Also, the on-ramp flow of the bottleneck section i is the minimum of the flow corresponding to the metering rate and the flow corresponding to the vehicles waiting in the on-ramp j plus the arriving vehicles (see (8)).

$$q_i^{in}(k) = \overline{q}_j^{in}(k) \tag{7}$$

$$q_i^{on}(k) = \min\left[r_j(k), d_j(k) + \frac{n_j(k)}{T}\right] \tag{8}$$

where r_j is the executed metering rate, d_j is the vehicle arriving rate, n_j is the initial vehicle number on the ramp, and T is the duration of one time step.

The system metering rate r_j' adopts the more restrictive of the bottleneck metering rate r_j^B and the local metering rate r_j^L.

$$r_j'(k+1) = \min\left[r_j^L(k+1), r_j^B(k+1)\right] \tag{9}$$

Then, the metering rate is adjusted to prevent the vehicle queue of each on-ramp exceeding the storage capacity N_j. The vehicle queue in the next time step is the initial vehicles on the ramp plus arriving vehicles and then minus released vehicles (see (10)). Thus deduce the minimum metering rate to satisfy the queue limits r_j^{queue} (see (11)).

$$n_j(k) + \left[d_j(k+1) - r_j(k+1)\right] T \le N_j \tag{10}$$

$$r_j^{queue}(k+1) = d_j(k+1) + \frac{n_j(k) - N_j}{T} \tag{11}$$

Besides, the metering rate should be no less than the preset minimum value r_j^{min}. Thus, the final metering rate is the maximum of r_j', r_j^{queue} and r_j^{min}.

$$r_j(k+1) = \max\left[r_j'(k+1), r_j^{queue}(k+1), r_j^{min}\right] \tag{12}$$

Finally, the metering rate is converted to green time g_j.

$$g_j(k+1) = \frac{r_j(k+1)}{r_j^{sat}} \times C_j \tag{13}$$

where r_j^{sat} is the saturation flow (usually 1800 pcu/h) and C_j is the signal cycle. Figure 2 presents the flow chart of the bottleneck algorithm described above.

3. Weights Calibration

3.1. Data Description. Data used in this research include trajectory data, loop detector data, and a corresponding road network map. Trajectory data is collected from a typical week, from 23 October 2017 to 29 October 2017, including about 13 million records. The indicators include a timestamp, vehicle ID, speed, location in terms of longitude, latitude, and road ID matched to the road network map. Vehicle trajectory data are collected by mobile navigation applications. They are a kind of crowd-sourced data. With the development of mobile Internet technology, a great number of drivers use mobile navigation applications such as Google Map and Amap during their trips. To provide real-time navigation service, these mobile applications frequently collect and update vehicle location and movement, as shown in Figure 3. Each vehicle is assigned an ID, with which its trajectory can be accurately reproduced. Mobile phones with these navigation applications are essentially mobile sensors. The vehicle trajectory data can be regarded as an improved version of floating car data with higher collection frequency and higher penetration.

Loop detector data cover the mainline and ramps of North-South Elevated Road in Shanghai, China. The duration is from 1 October 2017 to 31 October 2017. There are about 0.9 million records of traffic statistics in 5 minutes, including volume, occupancy, and speed. Detectors can be located to map via loop ID. Besides, the map contains information about the road network, such as road name, length, width, and number of lanes of the link.

3.2. Origin-Destination Extraction. Origins and destinations of trips can be extracted from vehicle trajectory data. Generally, trips are distinguished by different purposes. Vehicle trajectory is divided into multiple trips based on dwell time and dwell location [33]. In this research, the problem is discussed in freeway networks where vehicles normally keep moving. Also, trajectory is collected every 5 seconds on average, forming a chain of continuous records as shown in Figure 3. These advantages simplify the process of OD extraction. When a vehicle first appears in the freeway network, the corresponding record is regarded as the origin of a trip. The following records all belong to this trip until one record appears at a nonadjacent road or the time gap between this record and the previous sequence is large enough. Then this record signifies a new trip. Since normally there does not exist trip purposes on the freeway, the OD extraction algorithm only needs to examine temporal and spatial continuity for trajectory records in the same trip.

Figure 4 presents a flow chart to extract OD pairs from trajectory data. First, all trajectory data are ordered by vehicle ID and timestamp. The algorithm compares two contiguous records. If they have the same vehicle ID, their time gap is less than a threshold (e.g., 10 minutes), and the path is continuous, then these two records belong to the same trip and the temporary destination is updated to the latter record; otherwise, the former record is the destination of this trip and the latter record is the origin of a new trip. Figure 5 shows an example of ordered trajectory data. They are divided into several trips through Figure 4. In this way, the origin and the destination of each trip and their corresponding location and time are extracted.

3.3. Validation Test. In order to verify that the OD pairs extracted from trajectory data are representative samples, we count the number of vehicles passing through a link within a given time interval from trajectory data and count the flow volume of the same link within the same time interval from loop detector data. The former is sample since not all vehicles return trajectory data. Pearson correlation coefficient ρ is utilized to evaluate the linear correlation between the link counts extracted from trajectory data $X = \{x_1, \ldots, x_n\}$ and the link counts collected by loop detectors $Y = \{y_1, \ldots, y_n\}$, where n is the size of the statistics, which equals the link number times the interval number.

$$\rho = \frac{\sum_{i=1}^{n}(x_i - \overline{x})(y_i - \overline{y})}{\sqrt{\sum_{i=1}^{n}(x_i - \overline{x})^2}\sqrt{\sum_{i=1}^{n}(y_i - \overline{y})^2}} \tag{14}$$

ρ ranges from -1 to +1, where $\rho > 0$ is a positive correlation, $\rho < 0$ is a negative correlation, and 0 is no linear correlation. The larger $|\rho|$ indicates a stronger correlation. In general, $|\rho| \geq 0.7$ means a strong linear correlation. Trajectory data are regarded as representative samples if they pass this validation test.

3.4. Weights Calculation. Proper selection of weights is important to the control effect. If the volume reduction of a bottleneck is distributed too much to an on-ramp where vehicles do not destine for the bottleneck, then the metering rate is too restrictive. On the contrary, if too many vehicles are allowed into the freeway but they do not get off the freeway before the bottleneck; the metering rate is too loose. Accurate OD estimation provides valuable information for weights calculation [11]. In this research, the weights calculation is based on the OD patterns extracted from trajectory data. The traffic demand from one on-ramp to different destinations is the on-ramp demand times its destination choices proportion. Trajectory data provide representative samples of OD pairs to calculate this proportion. Let $d_{j,l}$ be the traffic demand from on-ramp j to destination l, $x_{j,l}$ be the corresponding number of trips extracted from trajectory data, and v be the number of destinations. Then,

$$d_{j,l} = d_j \cdot \frac{x_{j,l}}{\sum_{l=1,\ldots,v} x_{j,l}} \tag{15}$$

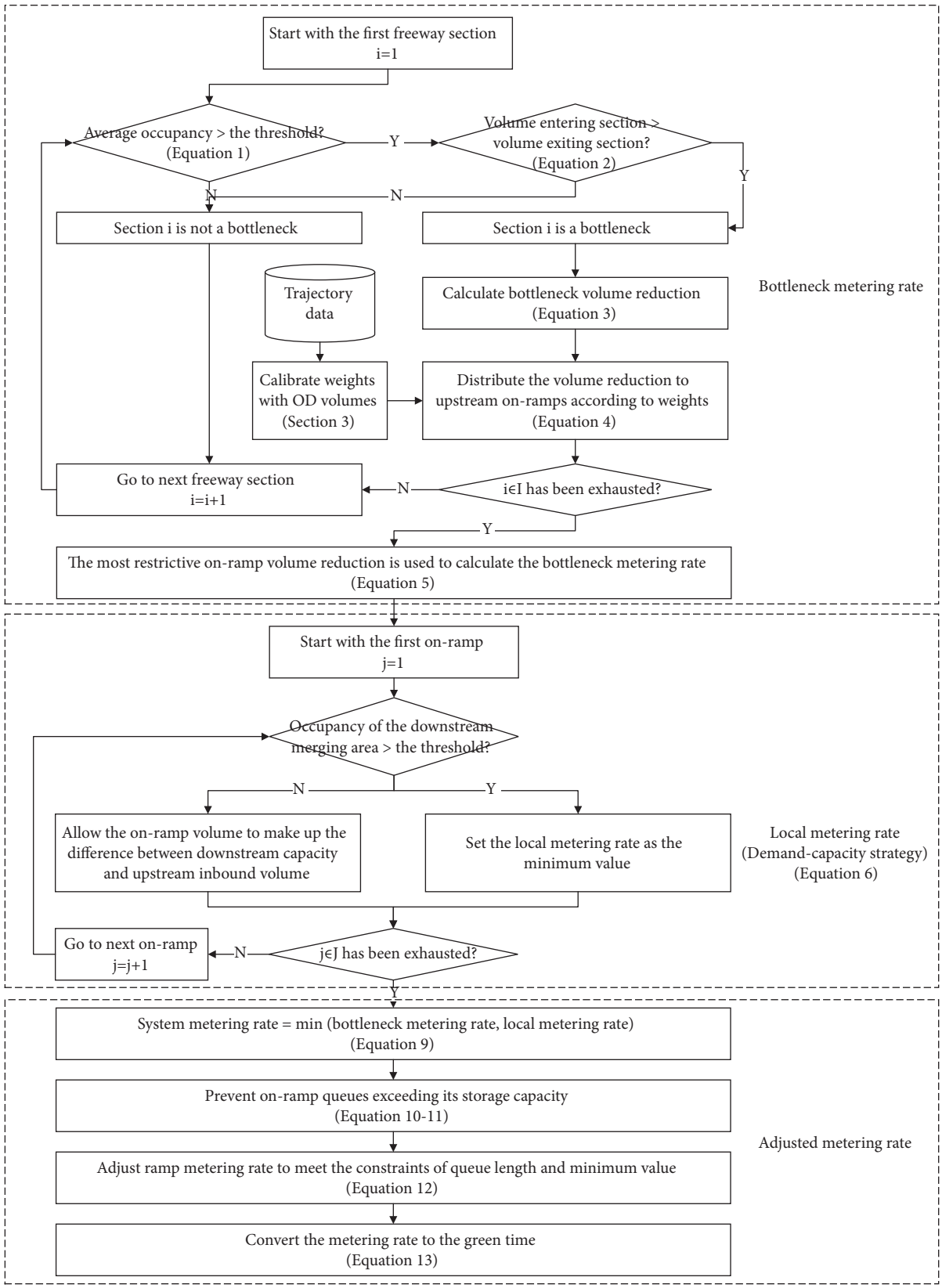

Figure 2: The flow chart of the bottleneck algorithm.

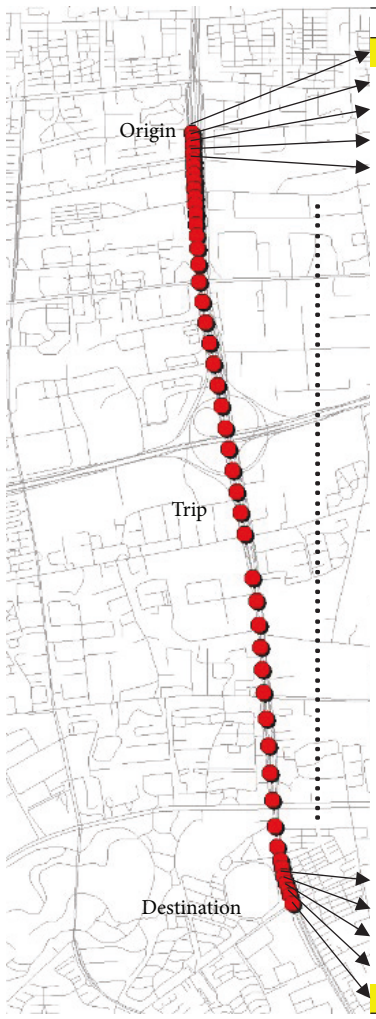

Timestamp	Vehicle ID	Speed	Longitude	Latitude	Road ID
2017/10/23 09:24:31	7197********	18	121.448647	31.303833	35935
2017/10/23 09:24:36	7197********	17	121.448662	31.303623	35935
2017/10/23 09:24:41	7197********	22	121.448677	31.303356	35935
2017/10/23 09:24:46	7197********	23	121.448685	31.303061	35935
2017/10/23 09:24:51	7197********	15	121.448700	31.302816	35935
2017/10/23 09:24:56	7197********	18	121.448708	31.302603	35935
2017/10/23 09:25:01	7197********	23	121.448715	31.302326	35935
2017/10/23 09:25:06	7197********	22	121.448730	31.302063	35935
2017/10/23 09:25:11	7197********	23	121.448746	31.301781	35935
2017/10/23 09:25:16	7197********	20	121.448761	31.301481	35935
2017/10/23 09:25:21	7197********	26	121.448776	31.301207	35935
2017/10/23 09:25:26	7197********	26	121.448792	31.300854	1511
2017/10/23 09:25:31	7197********	33	121.448814	31.300488	1511
2017/10/23 09:25:36	7197********	34	121.448837	31.300072	1511
2017/10/23 09:25:41	7197********	43	121.448860	31.299625	1511
.....	.....	...	.....	.....	.....
.....	.....	...	.....	.....	.....
.....	.....	...	.....	.....	.....
2017/10/23 09:27:21	7197********	68	121.451630	31.284294	35624
2017/10/23 09:27:26	7197********	73	121.451706	31.283442	35624
2017/10/23 09:27:31	7197********	81	121.451797	31.282478	36078
2017/10/23 09:27:36	7197********	81	121.451881	31.281490	36078
2017/10/23 09:27:41	7197********	80	121.451973	31.280516	36078
2017/10/23 09:27:46	7197********	80	121.452065	31.279539	36078
2017/10/23 09:27:51	7197********	77	121.452164	31.278564	35689
2017/10/23 09:27:56	7197********	59	121.452278	31.277803	35689
2017/10/23 09:28:01	7197********	48	121.452393	31.277313	35689
2017/10/23 09:28:06	7197********	32	121.452454	31.277052	35689
2017/10/23 09:28:16	7197********	12	121.452538	31.276754	35689
2017/10/23 09:28:26	7197********	11	121.452629	31.276491	35689
2017/10/23 09:28:48	7197********	7	121.452728	31.276247	35689
2017/10/23 09:29:16	7197********	6	121.452797	31.276056	35689
2017/10/23 09:29:31	7197********	10	121.452904	31.275770	35689

Figure 3: An example of vehicle trajectory data.

The traffic demand from on-ramp j to bottleneck i is calculated by the sum of $d_{j,l}$ where destination l locates downstream of bottleneck i.

$$d_{j,i} = \sum_{l} d_{j,l} \tag{16}$$

Weights $W_{j,i}$ are the weights of on-ramp j to the bottleneck i, proportional to traffic demand $d_{j,i}$.

$$W_{j,i} = \frac{d_{j,i}}{\sum_j d_{j,i}} \tag{17}$$

There exists $\sum_j W_{j,i} = 1$ for each bottleneck section. Weights matrix is as (18). u and m are, respectively, the number of on-ramps and bottlenecks.

$$W_{u\times m} = \begin{bmatrix} W_{1,1} & \cdots & W_{1,m} \\ & \ddots \quad \cdots \quad \ddots & \\ 0 & \vdots \quad W_{j,i} \quad \vdots & \vdots \\ & 0 \quad \cdots \quad \ddots & \\ 0 & 0 & W_{u,m} \end{bmatrix} \tag{18}$$

4. Simulation Experiments

4.1. Network Description. A real urban freeway in Shanghai is simulated using the microscopic simulation software PTV VISSIM. The freeway is of 7.5 km in length, with 4 on-ramps, 3 off-ramps, and freeway-to-freeway ramps. The north end locates at a suburban area and the south end is in downtown. Figure 6 annotates the length of mainline sections and on-ramps. The first and second row of the pictures shown in Figure 6, respectively, show on-ramps in the real world and in the simulation.

4.2. Simulation Settings. Experiments simulate freeway operation on weekdays' morning peak (7:00 – 10:00), a typical recurrent congestion scenario. Data of 24 October 2017 (Tuesday) are utilized to get simulation inputs of traffic demand patterns, as shown in Figure 7. Vehicle Inputs are derived from loop counts. Vehicle routes and their relative flows are set according to the OD patterns extracted from trajectory data. Besides, speed limits on mainlines and on ramps are respectively 80 km/h and 40 km/h, as in the real world.

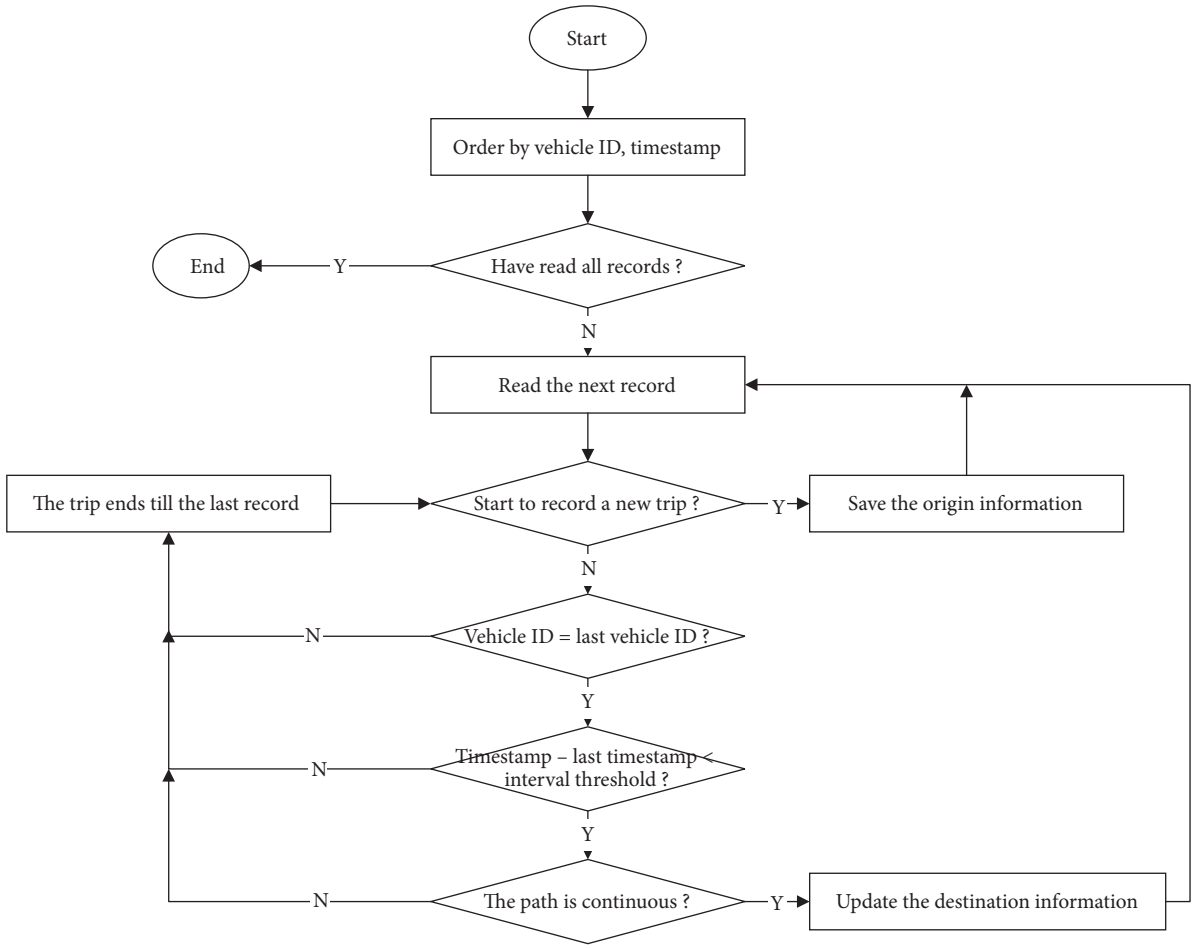

Figure 4: The flow chart of the algorithm to extract origin-destination from trajectory data.

4.3. Control Parameters Settings. Bottlenecks usually exist at merging areas downstream of on-ramps, weaving areas upstream of off-ramps and lane-drop areas. There are four bottlenecks in this freeway network. Figure 8 shows the relationship between occupancy o and flow q for each bottleneck. A sigmoidal function fits best [40].

$$q(o) = a \cdot c \cdot o \cdot \left(1 - \frac{1}{1 + e^{b - c \cdot o}}\right) \tag{19}$$

where a, b, c are all regression parameters. The occupancy threshold o^{thres} is set corresponding to the capacity flow. When $o^{thres} = [0.28, 0.27, 0.25, 0.22]$, the flow of the bottleneck section reaches the maximum of the fitted curve. In this freeway network, occupancy downstream of the on-ramp and occupancy of the bottleneck section are measured by the same loop detector. Thus, they have the same thresholds. In addition, for all controlled on-ramps, signal cycles C are 60s, saturation flow r^{sat} is 1800 pcu/h· lane, and minimum metering rate r^{min} is 60 pcu/h· lane.

4.4. Scenarios and Cases. The simulation experiments on three cases: (1) no control real-world case; (2) control with loop data—adopting a classic method "gravity model" to estimate OD with loop counts [25]; (3) control with trajectory data—implementing the proposed approach. Control schemes are conducted under three scenarios: (1) real-world traffic demand; (2) 20% less traffic demand for the mainline and all on-ramps; (3) 20% more traffic demand for the mainline and all on-ramps. Besides, to prepare simulation environments, there is no control for the first 15 minutes in all experiments. For each scenario and each case, we run 20 experiments with different random seeds and then take averages.

5. Results and Analysis

5.1. Linear Correlation. There exists a strong linear correlation between link counts from trajectory data (X) and those from loop data (Y), as shown in Figure 9. Their relation can be fitted as $X = 0.1347Y + 5.815$. This means the penetration of the trajectory data reaches 13.5%, much higher than traditional floating car data. Also, the Pearson correlation coefficient ρ is 0.8775. Thus, the trajectory data pass the validation test and can be used to calculate weights matrix.

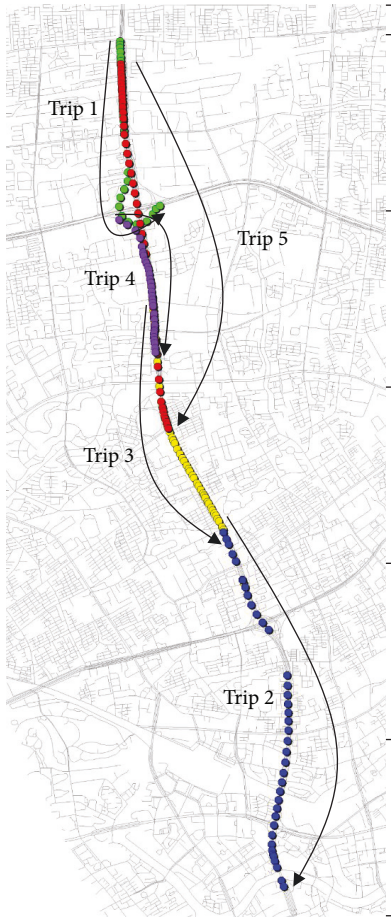

	Timestamp	Vehicle ID	Speed	Longitude	Latitude	Road ID
Trip 1	2017/10/23 09:16:06	2711********	21	121.448570	31.305573	35935
	2017/10/23 09:16:11	2711********	19	121.448578	31.305309	35935
	.....	.....	…	.....	.....	.....
	.....	.....	…	.....	.....	.....
	2017/10/23 09:19:42	2711********	34	121.451805	31.292656	8221
	2017/10/23 09:19:47	2711********	26	121.452164	31.292877	8221
Trip 2	2017/10/23 11:23:15	6445********	38	121.457848	31.267767	29633
	2017/10/23 11:23:20	6445********	56	121.458130	31.267225	29633
	.....	.....	…	.....	.....	.....
	.....	.....	…	.....	.....	.....
	2017/10/23 11:26:48	6445********	47	121.463089	31.240946	56742
	2017/10/23 11:26:53	6445********	45	121.463295	31.240458	56742
Trip 3	2017/10/23 17:47:09	6840********	53	121.448494	31.291805	663873
	2017/10/23 17:47:14	6840********	67	121.449203	31.291451	663873
	.....	.....	…	.....	.....	.....
	.....	.....	…	.....	.....	.....
	2017/10/23 17:52:09	6840********	24	121.451714	31.281918	31727
	2017/10/23 17:52:14	6840********	26	121.451744	31.281622	31727
Trip 4	2017/10/23 07:18:17	6952********	14	121.451492	31.285774	35624
	2017/10/23 07:18:27	6952********	20	121.451530	31.285332	35624
	.....	.....	…	.....	.....	.....
	.....	.....	…	.....	.....	.....
	2017/10/23 07:45:37	6952********	7	121.459595	31.264107	36073
	2017/10/23 07:45:47	6952********	10	121.459702	31.263847	36073
Trip 5	2017/10/23 09:24:31	7197********	18	121.448647	31.303833	35935
	2017/10/23 09:24:36	7197********	17	121.448662	31.303623	35935
	.....	.....	…	.....	.....	.....
	.....	.....	…	.....	.....	.....
	2017/10/23 09:29:16	7197********	6	121.452797	31.276056	35689
	2017/10/23 09:29:31	7197********	10	121.452904	31.275770	35689

Figure 5: An example of origins and destinations of trips extracted from vehicle trajectory data.

5.2. Weights Matrix. There are 4 on-ramps and 4 bottleneck sections, so the weights matrix is in the size of 4×4. Table 1 compares the results of the weights matrix generated from different data sources. Results show that the estimation with only loop data is more easily affected by ramp volumes. Taking the traffic contribution of bottleneck 2 for instance, the result attaches more importance to on-ramp 1 as it has much more volume than on-ramp 2. However, vehicle trajectories reveal that traffic entering from on-ramp 1 massively exits at the immediate downstream off-ramp (off-ramp 1) and does not reach bottleneck 2, because off-ramp 1 connects to another freeway. Similar results can be found in other bottleneck sections. With only fixed-location measurements, the OD estimation deviates more from the reality.

5.3. Mainline Performance. Experiments are performed under three scenarios and three cases. To evaluate the performance, 25 loop detectors are evenly placed on the mainline. The mainline is divided into 25 sections of 300 meters in length on average. Four on-ramps are, respectively, near section 3, 7, 15 and 24. Figure 10 presents mainline occupancies profiles of each experiment, and Table 2 lists performance indicators of average occupancy, average vehicle flow, and mean speed.

Real-world simulation is as in Figure 10(d); the most serious congestion appears in the bottleneck around on-ramp 4. The congestion spreads to upstream mainline over time. Congestion also forms in the rest three bottlenecks sometimes. The ramp metering control with loop data or trajectory data brings significant improvement, as shown in Figures 10(e) and 10(f). Their average occupancies are, respectively, reduced by 18% and 22%. Vehicle flows are increased by 2% and 6%. The congestion is reduced around the fourth bottleneck. It forms later and disappears earlier. Traffic condition is also improved in the rest mainline sections. Congestion is slightly reduced at the beginning and almost eliminated after 75 minutes.

When traffic demand reduces by 20%, traffic congestion only occurs at the fourth bottleneck. To eliminate the congestion, entering traffic is controlled at upstream on-ramps even if there is no congestion around these ramps. Mean speed increases by 5% but vehicle flow decreases by 8%. The control effect with loop data and with trajectory data is of little difference.

When traffic demand increases by 20%, traffic conditions become significantly worse in the first two bottleneck sections. The ramp control with loop data hardly improves the situation. In contrast, the control with trajectory data

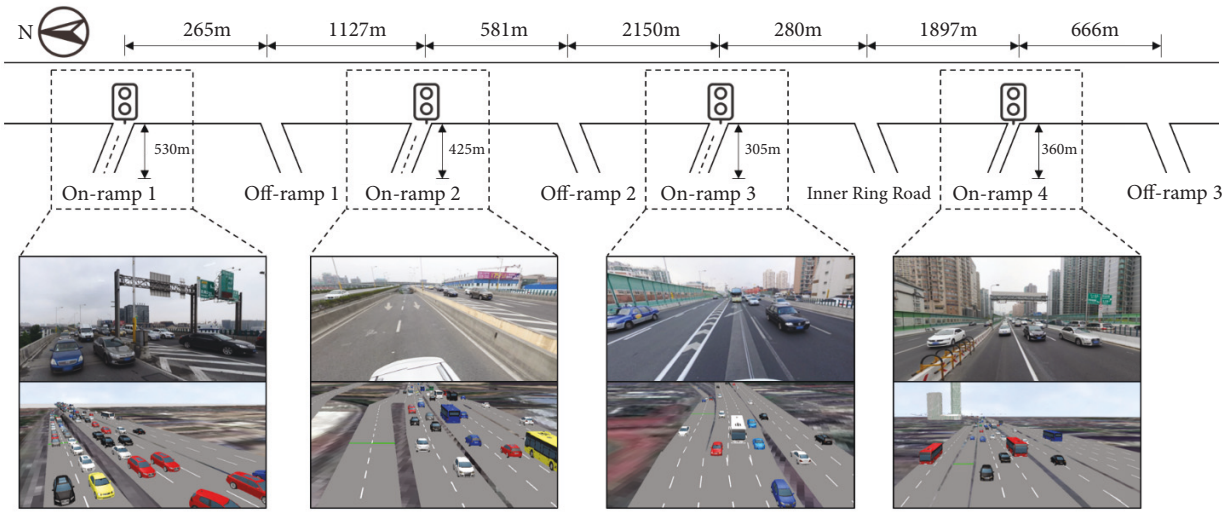

Figure 6: Test site with multiple ramps of North-South Elevated Road (southbound) in Shanghai, China.

Table 1: Weights matrix calculated with loop data and trajectory data.

		Bottleneck 1	Bottleneck 2	Bottleneck 3	Bottleneck 4
Loop data	On-ramp 1	1.00	0.87	0.38	0.16
	On-ramp 2	0.00	0.13	0.06	0.02
	On-ramp 3	0.00	0.00	0.56	0.24
	On-ramp 4	0.00	0.00	0.00	0.58
		Bottleneck 1	Bottleneck 2	Bottleneck 3	Bottleneck 4
Trajectory data	On-ramp 1	1.00	0.78	0.18	0.08
	On-ramp 2	0.00	0.22	0.05	0.02
	On-ramp 3	0.00	0.00	0.76	0.20
	On-ramp 4	0.00	0.00	0.00	0.70

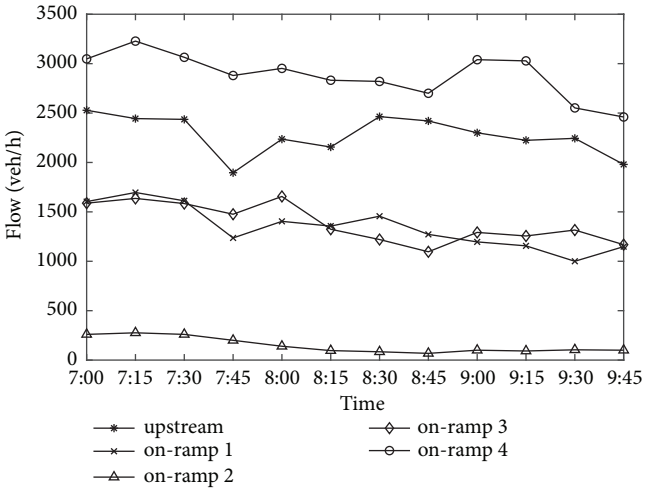

Figure 7: Traffic demand patterns of the test site.

shows better performance, because the control parameters of weights are selected more properly. The control effect is remarkable especially between section 10 and section 25, as more upstream entering traffic can be controlled by ramp metering. It even prevents bottleneck activation around on-ramp 3. Occupancy is reduced by 10% under the control with trajectory data, compared to a 3% reduction under the control with loop data. Vehicle flow and speed are both raised more with trajectory data.

5.4. Overall Travel Time. To reveal whether time saved on the mainline exceeds on-ramp delay caused by ramp metering, the simulation measures travel time of vehicles from different origins, i.e., the upstream mainline and four on-ramps, as shown in Figure 11. For demand level of 100%, the average travel time weighted by flow volume reduces by 19%. The travel time of upstream traffic is reduced by 29%, which means more than 4 minutes are saved for each trip. The travel time of vehicles entering from 4 on-ramps is reduced by 7%, 28%, 23%, and 16%, respectively.

For demand level of 80%, the travel time of traffic from on-ramp 1 and on-ramp 3 is increased by about 75%, which means ramp metering does not bring benefits for these vehicles. However, other traffic's travel time is saved a little. On average, travel time is increased by 33%. Controls with different data have little difference under these two scenarios.

For demand level of 120%, the average travel time is increased by 6% with loop data and reduced by 11% with

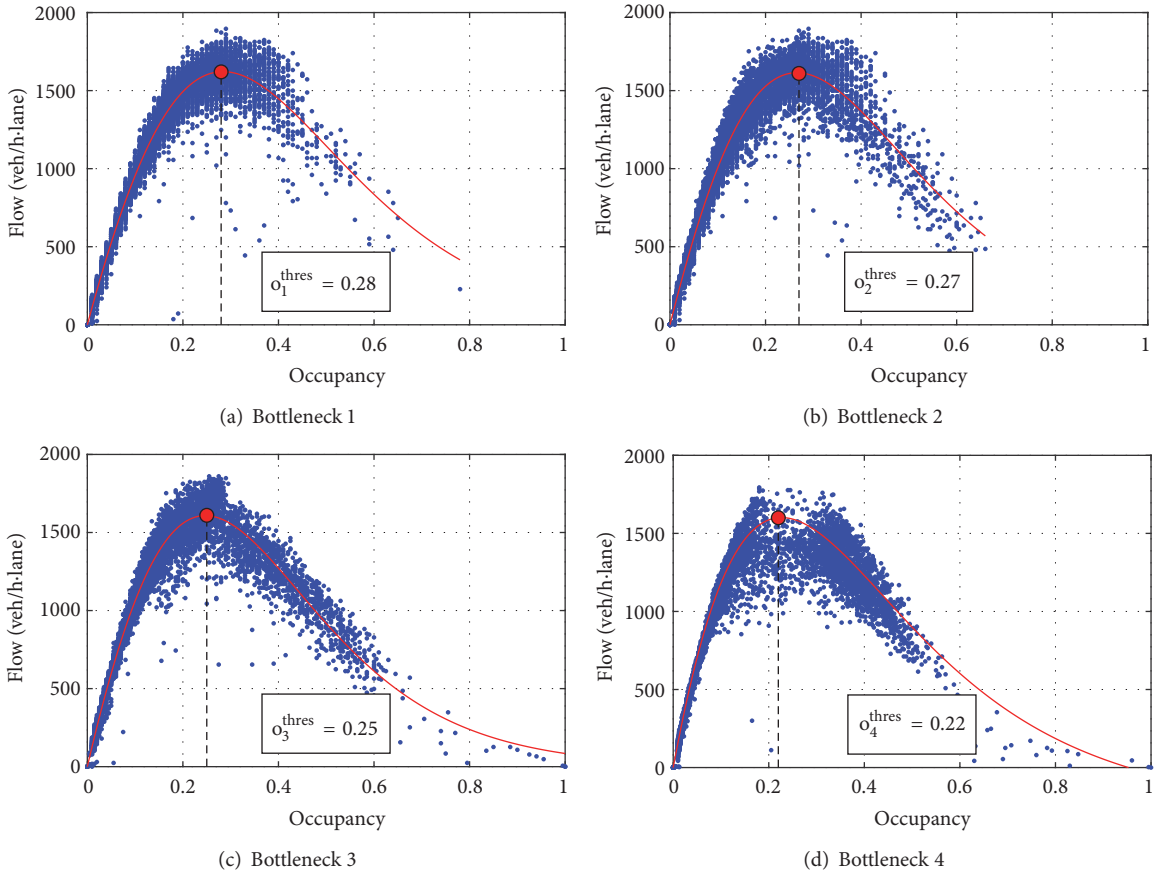

(a) Bottleneck 1 (b) Bottleneck 2

(c) Bottleneck 3 (d) Bottleneck 4

Figure 8: The relationship between occupancy and flow volume at four bottleneck sections.

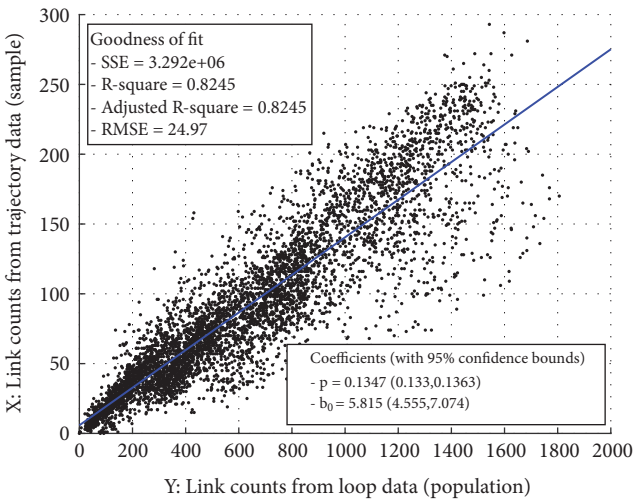

Figure 9: The linear relationship between link counts from trajectory data and those from loop data.

trajectory data. This result manifests significant advantage of ramp metering with trajectory data. It improves the mainline traffic operation, without the sacrifice of traffic from on-ramps.

6. Sensitivity Analysis

The penetration of trajectory data is supposed to influence the control effect. It is necessary to study its sensitivity on penetration rate and the minimum required value. A simple random sampling is used to lower the penetration rate. In order to reduce random noise, the sampling is done 50 times for each penetration rate and we take averages.

Figure 12(a) depicts the relationship between Pearson correlation coefficient ρ and the penetration rate p. With p decreasing, ρ reduces increasingly faster. We need to determine the critical penetration p_c, below which ρ drops significantly faster. The second-order difference $\Delta^2\rho$ is used to evaluate the changing speed of the descending slope. $\Delta^2\rho$ where $p \leq p_c$ should be significantly larger than $\Delta^2\rho$ where $p > p_c$. A t-test is applied to determine whether two groups of $\Delta^2\rho$ divided by p_c are significantly different from each other. When the penetration rate reduces to 4.0%, the t-test rejects the null hypothesis at the default 5% significance level; see Figure 12(b). The penetration of 4.0% is regarded as the minimum value, above which samples of vehicle trajectories are able to represent the characteristics of all vehicles and below which the reliability is not guaranteed.

Simulation experiments are performed under different penetration rates. Figure 13 compares indicators of

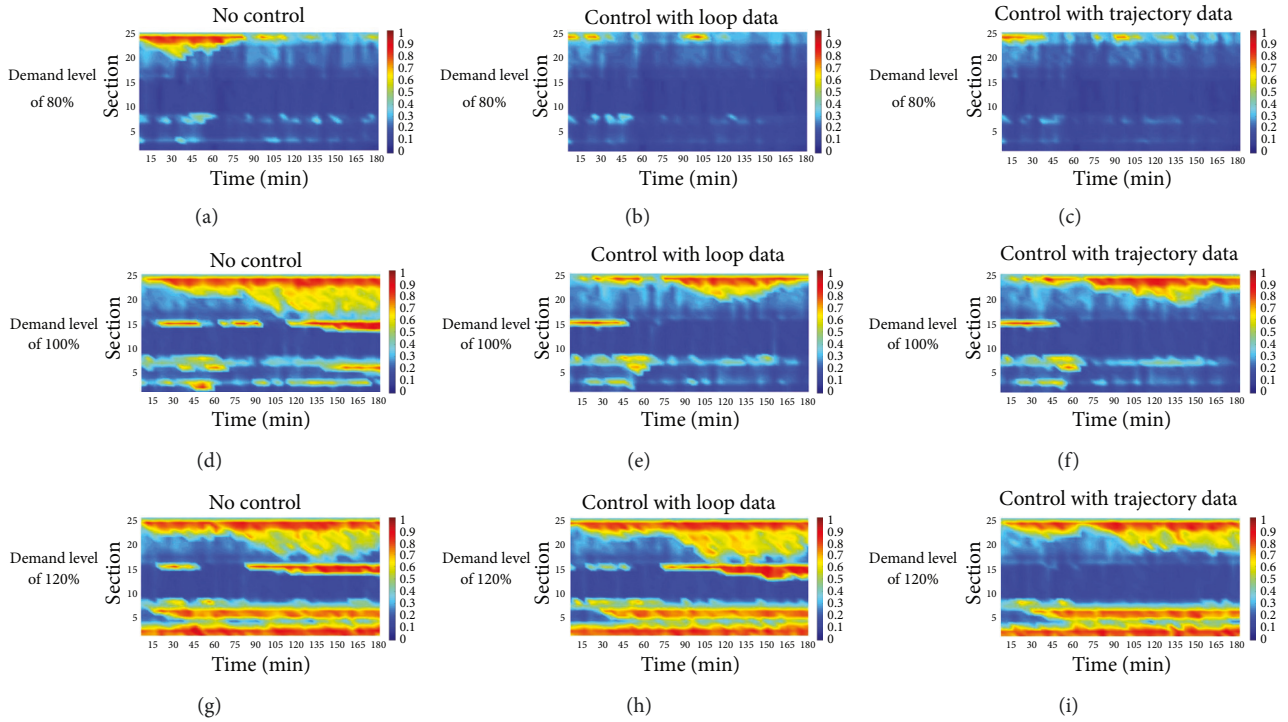

Figure 10: Mainline occupancies profiles.

Table 2: Mainline performance indicators.

Demand level	Cases	Occupancy		Vehicle flow		Speed	
		%	% change	veh/h	% change	km/h	% change
80%	No control	21.99	-	2466	-	68.64	-
	Control with loop data	18.76	-15%	2271	-8%	71.94	5%
	Control with trajectory data	18.06	-18%	2278	-8%	71.88	5%
100%	No control	35.74	-	2817	-	57.24	-
	Control with loop data	29.18	-18%	2883	2%	63.22	10%
	Control with trajectory data	27.90	-22%	2974	6%	65.48	14%
120%	No control	44.02	-	2616	-	50.01	-
	Control with loop data	42.55	-3%	2646	1%	50.97	2%
	Control with trajectory data	39.74	-10%	2743	5%	54.02	8%

occupancy, vehicle flow, and speed relative to the scenario of no control. Control effects get worse when penetration reduces. When the penetration rate is less than the minimum required value of 4.0%, the performance becomes more sensitive. The reason is that less penetration leads to less reliable results. When trajectory data volume is not sufficient, weight calibration tends to be improper and ramp metering becomes less effective in that way.

7. Conclusion

This paper extracts OD patterns from trajectory data, validates the representativeness of the sample vehicle trajectories, and applies the historical OD patterns to coordinated ramp metering. To verify its advantage, the bottleneck algorithm is implemented with different data sources—loop data (traditional control) and trajectory data (our approach). A real urban freeway is simulated to test control effects.

Simulation experiments show that ramp metering with trajectory data increases another 4% throughput compared to traditional control under current traffic demand. The advantage is more significant under heavier demand. When traditional control can hardly relieve the congestion and even increase average travel time by 6%, our approach increases throughput by 5% and reduces travel time by 11%. However, their control performance shows little difference under low demand. The reason is that trajectory data can help accurate estimation of traffic contribution for bottleneck sections. This information is more important to effective control when traffic condition is oversaturated. Also, the control performance is affected by the penetration of trajectory data. The

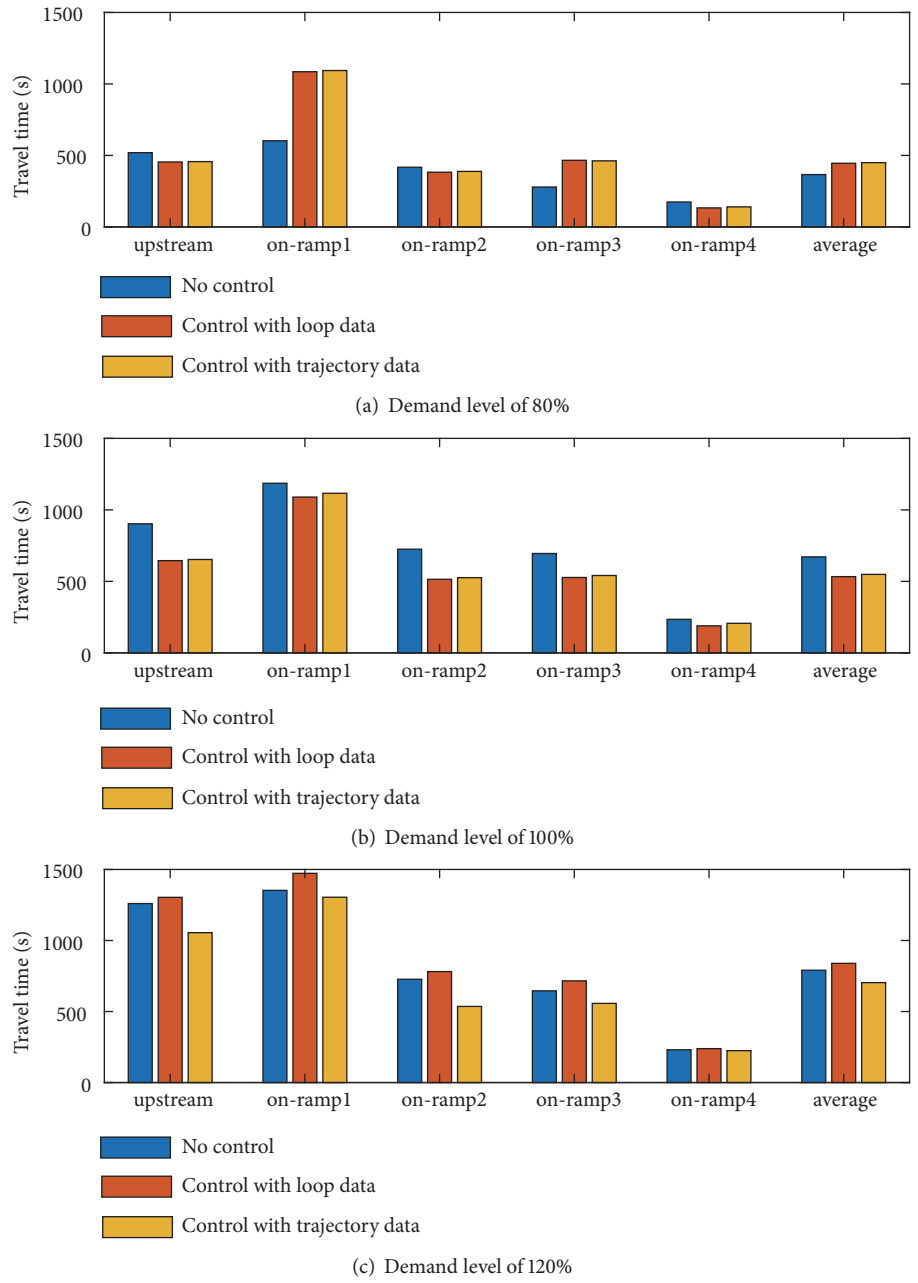

Figure 11: The travel time of vehicles from different origins.

minimum required penetration is 4.0%, below which the OD estimation tends to become unreliable, and correspondingly the control has no advantage over the traditional one.

The approach proposed in the paper is free of strong assumption and complex computing; hence it is ready for practice. Experiments simulate real road networks and traffic demand patterns. The experiments are more persuasive than those under virtual scenarios. However, there are some limitations of the proposed approach. The bottleneck metering rate is calculated only when bottlenecks have been detected. Also, there exists a time lag between control actions being taken and having effects to the bottlenecks. Thus, it is only suitable to alleviate recurrent freeway congestion with steady OD patterns.

Future researches plan to improve models by further utilizing information recorded by vehicle trajectories. Prediction can be included to activate control before congestion forming. Feedback modules can also be added to increase robustness.

Data Availability

The data used to support the findings of this study have not been made available due to data security.

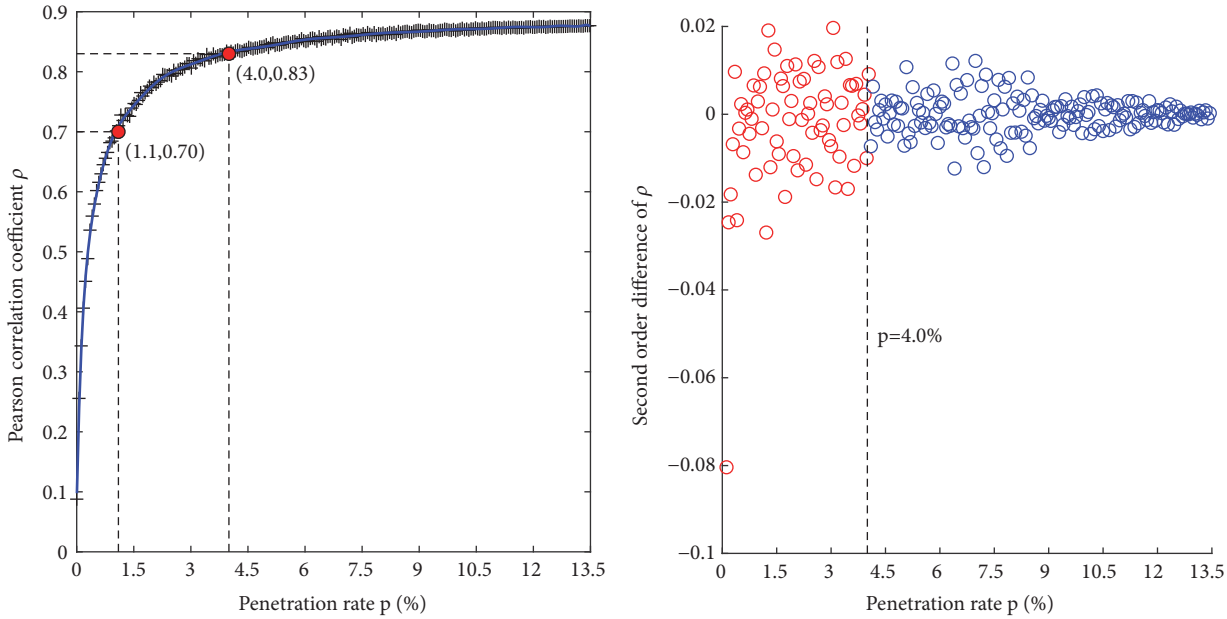

(a) The profile of ρ and p

(b) The profile of $\Delta^2\rho$ and p

FIGURE 12: The relationship between the Pearson correlation coefficient and the penetration rate.

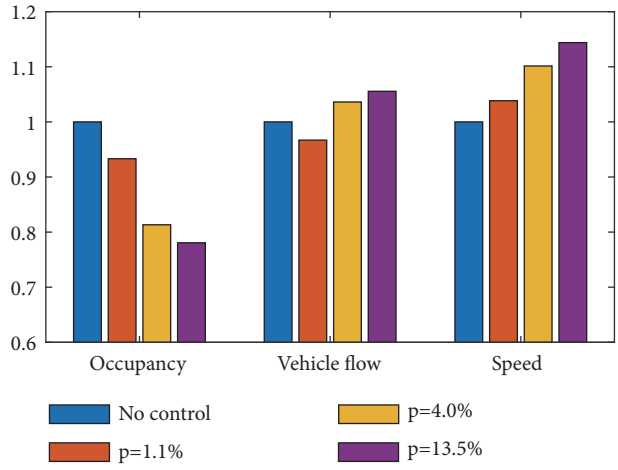

FIGURE 13: Mainline performance indicators under different penetrations.

Conflicts of Interest

The authors declare that there are no conflicts of interest regarding the publication of this paper.

Acknowledgments

This research was supported by National Natural Science Foundation of China (Grant no. 61773293), Shanghai Sailing Program (Grant no. 19YF1435100), Joint Laboratory for Future Transport and Urban Computing of AutoNavi, and Shanghai Transportation Information Center.

References

[1] M. Papageorgiou and A. Kotsialos, "Freeway ramp metering: an overview," *IEEE Transactions on Intelligent Transportation Systems*, vol. 3, no. 4, pp. 271–281, 2002.

[2] B. Persaud, S. Yagar, and R. Brownlee, "Exploration of the breakdown phenomenon in freeway traffic," *Transportation Research Record*, no. 1634, pp. 64–69, 1998.

[3] J. A Wattleworth, "Peak-period analysis and control of a freeway system," *Highway Research Records*, vol. 157, no. 9, pp. 1–21, 1965.

[4] D. P. Masher, D. W. Ross, P. J. Wong et al., "Guidelines for design and operation of ramp control systems," Standford Research

Institute Report NCHRP 3-22, SRI Project 3340, SRI, Menid Park, California, 1975.

[5] H. Hadj-Salem, J. M. Blosseville, and M. Papageorgiou, "ALINEA: a local feedback control law for on-ramp metering; a real-life study," in *Proceedings of the 3rd International Conference on Road Traffic Control*, pp. 194–198, London, UK, May 1990.

[6] M. Papageorgiou, H. Hadj-Salem, and F. Middelham, "ALINEA local ramp metering: summary of field results," *Transportation Research Record*, no. 1603, pp. 90–98, 1997.

[7] Y. Kan, Y. Wang, M. Papageorgiou, and I. Papamichail, "Local ramp metering with distant downstream bottlenecks: A comparative study," *Transportation Research Part C: Emerging Technologies*, vol. 62, pp. 149–170, 2016.

[8] Z. Hou, X. Xu, J. Yan, J.-X. Xu, and G. Xiong, "A complementary modularized ramp metering approach based on iterative learning control and ALINEA," *IEEE Transactions on Intelligent Transportation Systems*, vol. 12, no. 4, pp. 1305–1318, 2011.

[9] L. E. Lipp, L. J. Corcoran, and G. A. Hickman, "Benefits of central computer control for denver ramp-metering system," *Transportation Research Record*, vol. 1320, pp. 3–6, 1991.

[10] I. Papamichail, M. Papageorgiou, V. Vong, and J. Gaffney, "Heuristic ramp-metering coordination strategy implemented at monash freeway, Australia," *Transportation Research Record*, vol. 2178, pp. 10–20, 2010.

[11] L. N. Jacobson, K. C. Henry, and O. Mehyar, "Real-time metering algorithm for centralized control," *Transportation Research Record*, vol. 1232, pp. 17–26, 1989.

[12] Y. Stephanedes, "Implementation of on-line zone control strategies for optimal ramp metering in the minneapolis ring road," in *Proceedings of the Seventh International Conference on Road Traffic Monitoring and Control*, pp. 181–184, London, UK, 1994.

[13] G. Paesani, J. Kerr, P. Perovich, and F. E. Khosravi, "System wide adaptive ramp metering (SWARM)," *Merging the Transportation and Communications Revolutions. Abstracts for ITS America Seventh Annual Meeting and Exposition, Accession No 00744538*, 1997.

[14] M. Papageorgiou, "A new approach to time-of-day control based on a dynamic freeway traffic model," *Transportation Research Part B: Methodological*, vol. 14, no. 4, pp. 349–360, 1980.

[15] X. Yang, P. Yang, and Y. Iida, "A Study of dynamic traffic control for urban expressway," *China Journal of Highway and Transport*, vol. 11, no. 2, pp. 78–85, 1998.

[16] T. Yoshino, T. Sasaki, and T. Hasegawa, "The traffic-control system on the hanshin expressway," *Interfaces*, vol. 25, no. 1, pp. 94–108, 1995.

[17] I. Papamichail, A. Kotsialos, I. Margonis, and M. Papageorgiou, "Coordinated ramp metering for freeway networks: a model-predictive hierarchical control approach," *Transportation Research Part C: Emerging Technologies*, vol. 18, no. 3, pp. 311–331, 2010.

[18] M. Schmitt, C. Ramesh, and J. Lygeros, "Sufficient optimality conditions for distributed, non-predictive ramp metering in the monotonic cell transmission model," *Transportation Research Part B: Methodological*, vol. 105, pp. 401–422, 2017.

[19] T. Chang and Z. Li, "Optimization of mainline traffic via an adaptive co-ordinated ramp-metering control model with dynamic OD estimation," *Transportation Research Part C: Emerging Technologies*, vol. 10, no. 2, pp. 99–120, 2002.

[20] J. R. D. Frejo and E. F. Camacho, "Global versus local MPC algorithms in freeway traffic control with ramp metering and variable speed limits," *IEEE Transactions on Intelligent Transportation Systems*, vol. 13, no. 4, pp. 1556–1565, 2012.

[21] T. Jiang and X. Liang, "Fuzzy self-adaptive PID controller for freeway ramp metering," in *Proceedings of the 2009 International Conference on Measuring Technology and Mechatronics Automation, ICMTMA 2009*, pp. 570–573, China, 2009.

[22] H. Zhang, S. G. Ritchie, and R. Jayakrishnan, "Coordinated traffic-responsive ramp control via nonlinear state feedback," *Transportation Research Part C: Emerging Technologies*, vol. 9, no. 5, pp. 337–352, 2001.

[23] D. Zhao, X. Bai, F.-Y. Wang, J. Xu, and W. Yu, "DHP method for ramp metering of freeway traffic," *IEEE Transactions on Intelligent Transportation Systems*, vol. 12, no. 4, pp. 990–999, 2011.

[24] A. E. Willis and A. D. May, "Deriving origin-destination information from routinely collected traffic counts," Research Report, Institute of Transportation Studies, University of California, 1981.

[25] N. L. Nihan, "Procedure for estimating freeway trip tables," *Journal of the Transportation Research Board*, no. 895, Paper No HS-035 368, 1982.

[26] P. W. Lin and G. L. Chang, "A generalized model and solution algorithm for estimation of the dynamic freeway origin-destination matrix," *Transportation Research Part B: Methodological*, vol. 41, no. 5, pp. 554–572, 2007.

[27] H. D. Sherali and T. Park, "Estimation of dynamic origin-destination trip tables for a general network," *Transportation Research Part B: Methodological*, vol. 35, no. 3, pp. 217–235, 2001.

[28] C. Xie, K. M. Kockelman, and S. T. Waller, "A maximum entropy-least squares estimator for elastic origin-destination trip matrix estimation," *Procedia-Social and Behavioral Sciences*, vol. 17, pp. 189–212, 2011.

[29] E. Castillo, J. M. Menéndez, S. Sánchez-Cambronero, A. Calviño, and J. M. Sarabia, "A hierarchical optimization problem: estimating traffic flow using gamma random variables in a bayesian context," *Computers & Operations Research*, vol. 41, no. 1, pp. 240–251, 2014.

[30] R. Ásmundsdóttir, *Dynamic OD Matrix Estimation Using Floating Car Data*, Delft University of Technology, 2008.

[31] X. Yang, Y. Lu, and W. Hao, "Origin-destination estimation using probe vehicle trajectory and link counts," *Journal of Advanced Transportation*, vol. 2017, Article ID 4341532, 18 pages, 2017.

[32] S. M. Eisenman and G. F. List, "Using probe data to estimate OD matrices," in *Proceedings of the 7th International IEEE Conference on Intelligent Transportation Systems (ITSC '04)*, pp. 291–296, Washington, DC, USA, October 2004.

[33] W. Rao, Y. Wu, J. Xia, J. Ou, and R. Kluger, "Origin-destination pattern estimation based on trajectory reconstruction using automatic license plate recognition data," *Transportation Research Part C: Emerging Technologies*, vol. 95, pp. 29–46, 2018.

[34] J. B. Bugeda, L. M. Mercadé, L. Marqués, and C. Carmona, "A Kalman-filter approach for dynamic OD estimation in corridors based on bluetooth and Wi-Fi data collection," in *Proceedings of the 12th World Conference on Transportation Research*, 2010.

[35] Y. Cheng, X. Qin, J. Jin, B. Ran, and J. Anderson, "Cycle-by-cycle queue length estimation for signalized intersections using sampled trajectory data," *Transportation Research Record*, vol. 2257, no. 1, pp. 87–94, 2011.

[36] A. Thiagarajan, L. Ravindranath, K. LaCurts et al., "VTrack: accurate, energy-aware road traffic delay estimation using mobile phones," in *Proceedings of the 7th ACM Conference on Embedded Networked Sensor Systems (SenSys '09)*, pp. 85–98, November 2009.

[37] E. Jenelius and H. N. Koutsopoulos, "Travel time estimation for urban road networks using low frequency probe vehicle data," *Transportation Research Part B: Methodological*, vol. 53, pp. 64–81, 2013.

[38] L. Zhang and D. Levinson, "Optimal freeway ramp control without origin-destination information," *Transportation Research Part B: Methodological*, vol. 38, no. 10, pp. 869–887, 2004.

[39] M. Kontorinaki, I. Karafyllis, M. Papageorgiou, and Y. Wang, "An adaptive control scheme for local and coordinated ramp metering," in *Proceedings of the 20th IEEE International Conference on Intelligent Transportation Systems, ITSC 2017*, pp. 1–7, Japan, October 2017.

[40] Z. Zhang, S. A. Parr, H. Jiang, and B. Wolshon, "Optimization model for regional evacuation transportation system using macroscopic productivity function," *Transportation Research Part B: Methodological*, vol. 81, pp. 616–630, 2015.